Lasers in Manufacturing Conference 2021

Effect of microstructure for additively manufactured Ti64 plate on modulated pulses by vacuum SLM

Yuta Mizuguchi[a,*], Tuneyoshi Arimura[b], Masahiro Ihama[a], Yuji Sato[c], Norio Yoshida[c], Minoru Yoshida[b], Masahiro Tsukamoto[c]

[a]*Graduate School of Engineering, Osaka University, 1-1 Yamadaoka, Suita, Osaka, 565-0871, Japan*
[b]*Graduate School of Science and Engineering, Kindai University, 3-4-1 Kowakae, Higasiosaka, Osaka, 577-8502, Japan*
[c]*Joining and Welding Research Institute, Osaka University, 11-1 Mihogaoka, Ibaraki, Osaka, 567-0047, Japan*

Abstract

Selective Laser Melting (SLM), one of additive manufacturing technologies, can fabricate complex shapes such as lattice structures, porous structures, and biological structures. In addition, the ability to create the final shape allows for cost reduction and weight reduction of parts. Since the laser is irradiated layer by layer, the lower layers are affected by heat. As heat accumulates, the temperature of the entire object increases, and the aging effect promotes the growth of crystal grains in the lower layer, resulting in anisotropy in the object. In this study, we attempted to control the grain size by precisely controlling the amount of heat input for each layer in the layer-by-layer fabrication of Ti64 plates. The amount of heat input was controlled using a modulated pulsed laser. One layer was formed by changing the frequency of the modulation pulse, and the effects on the surface system and crystal grains of the formed object were investigated. As a result, the surface roughness increased and the grain size decreased as the frequency increased. A 10-layer Ti64 sample was fabricated and compared with samples fabricated using a modulated pulse laser and a continuous wave (CW) laser. The results showed that the grain uniformity of the samples fabricated using the modulated pulse laser was higher than that of the samples fabricated using the CW laser. This suggests that it is possible to control the material structure by modulated pulse laser.

Keywords: SLM; Heat input; Modulated pulses; Pulse energy; Grain size

1. Introduction

In recent years, an additive manufacturing technology has been attracting attention for its ability to freely fabricate ee three-dimensional shapes. The selective laser melting (SLM), one of the additive manufacturing, is a method of three-dimensional fabrication by melting and solidifying powders by laser irradiation and repeating this process. It is possible to form complex shapes such as lattices, porous structures, and biological

* Corresponding author.
E-mail address: mizuguchi@jwri.osaka-u.ac.jp.

structures. In addition, the ability to form the final shape allows for cost reduction and weight reduction of parts (Santos et al., 2006). Because of its potential, the market for SLM is expanding year by year. It is expected to be applied to automobiles, aerospace, and regenerative medicine such as artificial bones and joints. SLM technology is applicable to many kinds of materials, such as Ni-Fe (Zhang et al., 2013), Ti-N-Ti_5Si_3(Du et al., 2009), Ti-Al-C (Gu et al., 2009), Mg alloys (Gieseke et al., 2013), Al-Si-Mg alloys (Zhang et al., 2016), and IN718 (Wang et al., 2012). A group at the Lawrence Livermore National Laboratory in the U.S. has investigated the melting and solidification of powder in the SLM process in detail using numerical calculations, and clarified the mechanism of sputtering that occurs when the powder is irradiated by a laser. It was resulted these numerical calculations, they formed 316L stainless steel, which is two to three times stronger than conventional stainless steel and has the same ductility as conventional stainless steel (Wang et al., 2017). In the case of titanium alloys, Sun et al. formed Ti64 powder by the SLM method to form a porous structure (Sun et al., 2013), and Chunlei et al. formed Ti64 by the SLM method and evaluated the formed samples by X-ray diffraction (XRD) and scanning electron microscopy (SEM) (Chunlei et al., 2013). Zhang et al. formed pure Ti under vacuum and found that the surface roughness depended on the laser sweep speed (Zhang et al., 2013). In addition, Sato et al. have shown that the amount of spatter generation can be reduced and the surface accuracy can be improved by performing swept laser irradiation with appropriate parameters under vacuum (Sato et al., 2016). These reports suggest that in the SLM process, the laser as a heat source closely influences the mechanical properties of the formed object. However, there have been no reports of attempts to control the material structure or mechanical properties by controlling the heat input of the laser. In SLM process, the lower layer is affected by heat since the laser is irradiated layer by layer. Accumulation of heat raises the temperature of the entire object and the aging effect promotes the grain growth of crystal grains in the lower layer resulting in anisotropy of the fabricated object. In this study, we tried to control the grain size by precisely controlling the amount of heat input per layer for Ti64 plate additively fabrication. The Ti64 is widely used in several industries such as the automotive industry, chemical plants, petrochemical industry, etc. due to its excellent properties such as biocompatibility, high corrosion and erosion resistance, and mechanical resistance. The amount of heat input was controlled by using a modulated pulsed laser. The effect of the modulated pulse laser on the formed object was clarified by surface and cross-sectional observations of the fabricated object. In a previous study, monolayer fabrication using modulated pulse and CW lasers was performed and grain size reduction was confirmed (Mizuguchi et al., 2020). In this paper, we describe the effect of the modulation pulse frequency on the grain size and the effect of the modulated pulses on multi-layer fabrication.

2. Experimental procedures

2.1. Materials

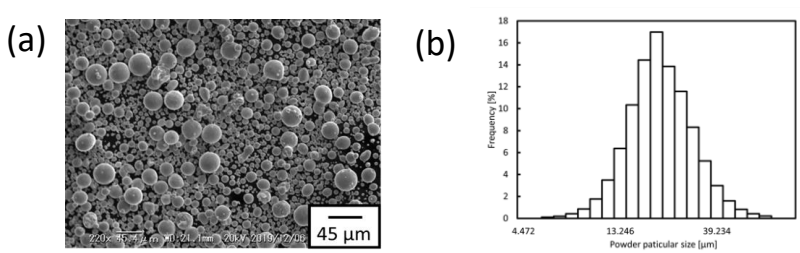

Fig. 1. (a) SEM image of Ti64 powder; (b) Particle size distribution of Ti64 powder

In this experiment, Ti64 powder (TILOP64-45, Osaka Titanium Technologies Co., Ltd.) was used. Fig. 1(a) shows the SEM (KEYENCE CORPORATION, VE-9800) image of the Ti64 powder used in this experiment. The

Ti64 powder was produced by gas atomization and was spherical in shape, and its particle size was distributed. In order to investigate the distribution, the particle size distribution of the powder materials was measured using a scattering particle size analyzer (LA-920, Horiba). Fig. 1(b) shows the particle size distribution of Ti64 powder. The grain size ranged from 5.867 to 67.523 µm, and the median of grain size was 19.904 µm. 3 mm thick pure Ti substrate was used.

2.2. Experimental setup for Ti64 fabricated with SLM in vacuum

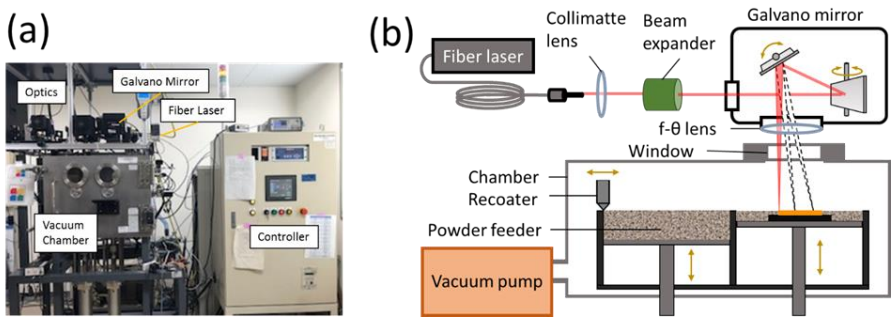

Fig. 2. (a) photo image of vacuum SLM equipment; (b) schematic diagram of experimental setup for vacuum SLM

Figure 2 shows a photo image and schematic diagram of the vacuum SLM experimental setup. A single-mode fiber laser (FITEL, Furukawa Electric Co., Ltd.) with a wavelength of 1084 nm and a maximum output power of 300 W was used for the SLM. The light emitted from the fiber laser was collimated by a collimating lens, the beam diameter was doubled by a beam expander, and the beam was focused and swept onto the fabrication surface through a two-axis galvano mirror and an f-θ lens. Figure 3 shows the beam profile on the fabrication surface using a USB 2.0 camera (IMAGINGSOURCE) with 1.2 megapixels and a pixel size of 3.75 µm × 3.75 µm. The intensity of the beam had a Gaussian distribution.

Table 1 shows the experimental conditions for this experiment. The experimental parameters were set to continuous wave (CW) and modulated pulses. The frequency of the modulated pulses was 100 Hz. The duty ratio was set to 50%. The laser sweep speed was 10 mm/s. The laser power was set to 300 W, and the spot diameter was set to 100 µm at $1/e^2$. The laser sweep method was employed the linear raster scan method, as shown in Fig. 4, and the hatching distance was set to 50 µm. The chamber was evacuated to 1.0×10^{-3} Pa to prevent from oxidation of Ti64 powder. Under these conditions, the powder was spread to a thickness of 50 µm, and single layer of 10 mm x 10 mm x 0.1 mm were fabricated. The surface system was evaluated by measuring the surface roughness Ra of the fabricated sample. The sample were cut in parallel with the direction of the laser sweep using micro cutter. Etching test was performed using Kroll's solution (mixture of 3 ml of 46% HF, 3 ml of 69% H_2SO_3, and 100 ml of distilled water) for evaluation of grain size by optical microscope (KEYENCE) observation. The grain size was measured by measuring the long side of the grain at two points in the microscope image. 50 points were measured, and the average value was taken.

Next, the experimental parameters were continuous wave (CW) and modulated pulse, and 10 layers of 10 mm x 10 mm x 0.5 mm were fabricated. After cutting and polishing the molding, the cross section was corroded to observe the crystal grains. The grain size was measured by measuring two points on the long side of the grain in the microscope image. Fifty points were measured, and the average value was taken.

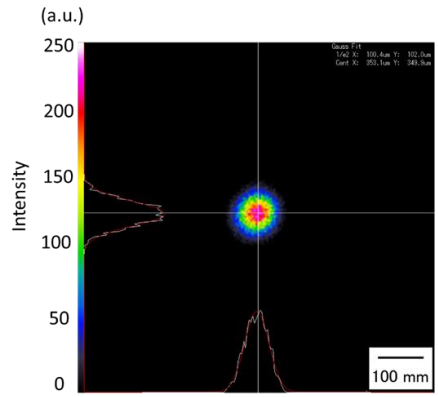

Fig. 3. Image of laser beam profile at the fabrication surface

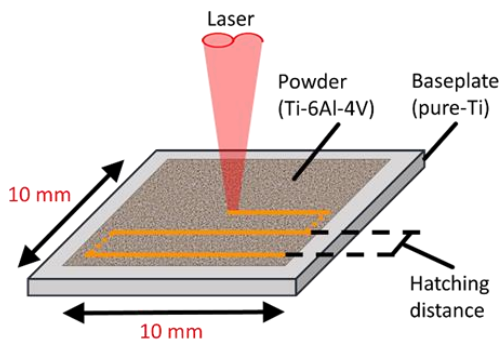

Fig. 4. Schematic diagram of the single bead formation

Table 1. Experimental condition of laser irradiation

Parameters	Value
Frequency (Hz)	100, 200, 400, 500, 800, 1000
Duty ratio (%)	50
Output power (W)	300
Wavelength (nm)	1084
Spot diameter (μm)	100
Scanning speed (mm/s)	10
Hatching distance (μm)	50
Layer thickness (μm)	50
Total layer number	10
Pressure in chamber (Pa)	1.0×10^{-3}

3. Results

3.1 Correlation between surface roughness, grain size and pulse energy in single layer fabrication

Figure 5 shows the optical microscope images of the surface of the formed object when the powder was irradiated by laser at each frequency. The surface roughness became rougher as the frequency increased. The measurement results of surface roughness Ra are shown in Fig. 6 At a frequency of 100 Hz, the surface roughness Ra was 3.21 µm, and the surface roughness Ra increased as the frequency increased.

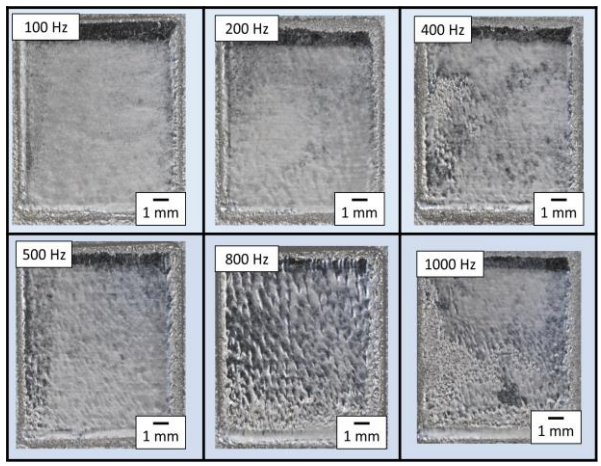

Fig. 5. Optical microscopy images of fabricated object

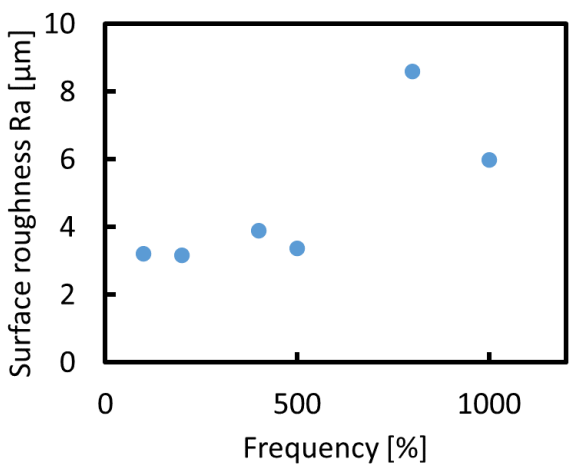

Fig. 6. Correlation between pulse frequency and surface roughness Ra.

An optical microscope image of the cross-section of the formed object is shown in Fig. 7. It can be confirmed that the crystal grains become finer as the frequency increases. The results of the grain size measurement are shown in Fig. 8. At a frequency of 100 Hz, the average grain size was 37.01 µm. The grain size tended to decrease as the frequency increased. From the above results, it is clear that increasing the frequency of the modulation pulse increases the surface roughness and decreases the grain size.

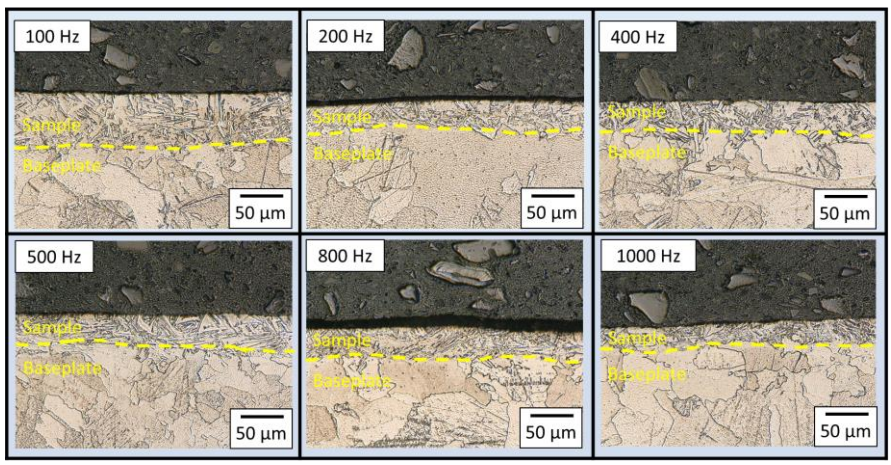

Fig. 7. Optical microscopy images of cross section perpendicular to the laser scanning line

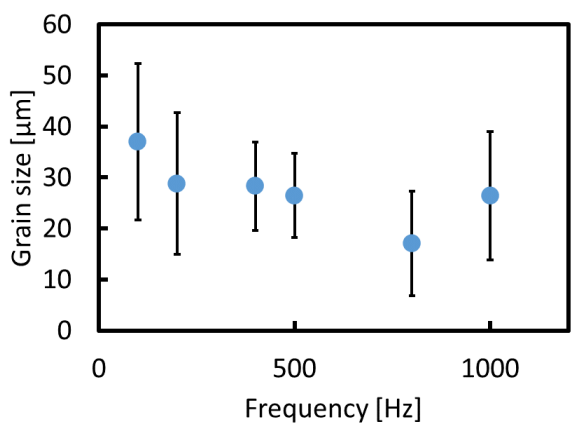

Fig. 8. Correlation between pulse frequency and grain size.

3.2 Grain distribution in multi-layer fabrication with modulated pulses

A modulated pulse laser with a frequency of 100 Hz and a duty ratio of 50% was used to create 10 layers sample. As a comparison, we fabricated a similar object using a CW laser. Fig. 9(a) and Fig. 9(b) show the objects formed by using CW laser and modulated pulsed laser, respectively. The surface roughness Ra was 10.6µm for the CW laser, and 6.32µm for the modulated pulse laser. The modulated pulse laser produced objects with a smoother surface.

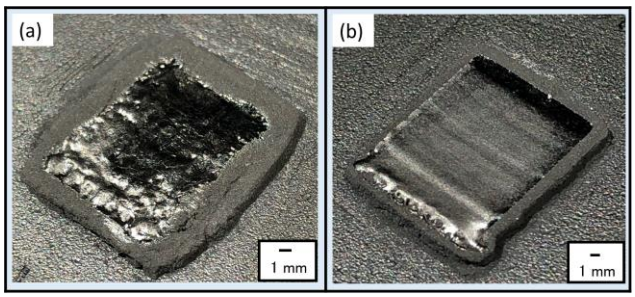

Fig. 9. Photo image of fabricated sample with (a) CW laser and (b) modulated pulsed laser

Fig. 10(a) and Fig. 10(b) shows the optical microscope images of the cross-section of the formed object when the CW laser and the modulated pulse laser were swept. The grain size was 107.24 µm for the CW laser and 38.96 µm for the modulated pulse laser. Fig. 11(c) to (f) show the optical microscope images of (a) and (b) near the surface and near the substrate. The grain size was measured in the range of 100 µm from the surface and 100 µm from the substrate, respectively. As shown in Fig. 12, the average grain size near the surface was 94.9 µm, and that near the substrate was 119.58 µm. The difference between the average grain size near the surface and that near the substrate was 24.68 µm. The difference between the grain diameters near the surface and near the substrate was 24.68 µm. The grain diameters near the surface and near the substrate were on average 34.94 µm and 42.97 µm, respectively, and the difference was 8.03 µm, which was smaller than that of the CW laser.

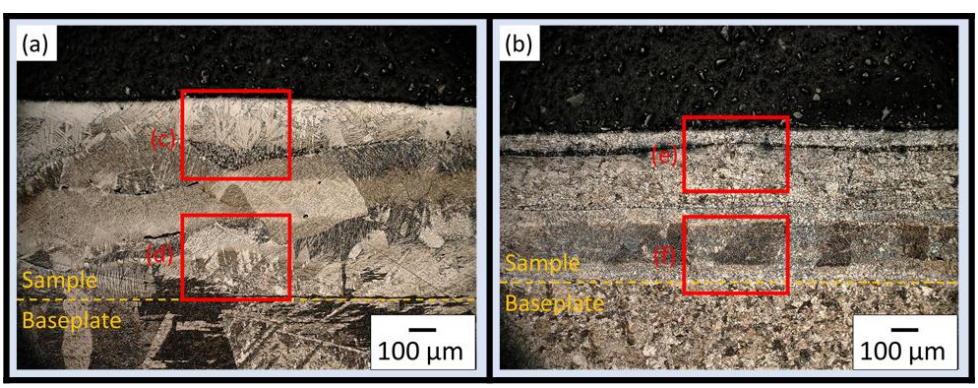

Fig. 10. Optical microscopy images of cross section perpendicular to the laser scanning line with (a) CW laser and (b) modulated pulsed laser.

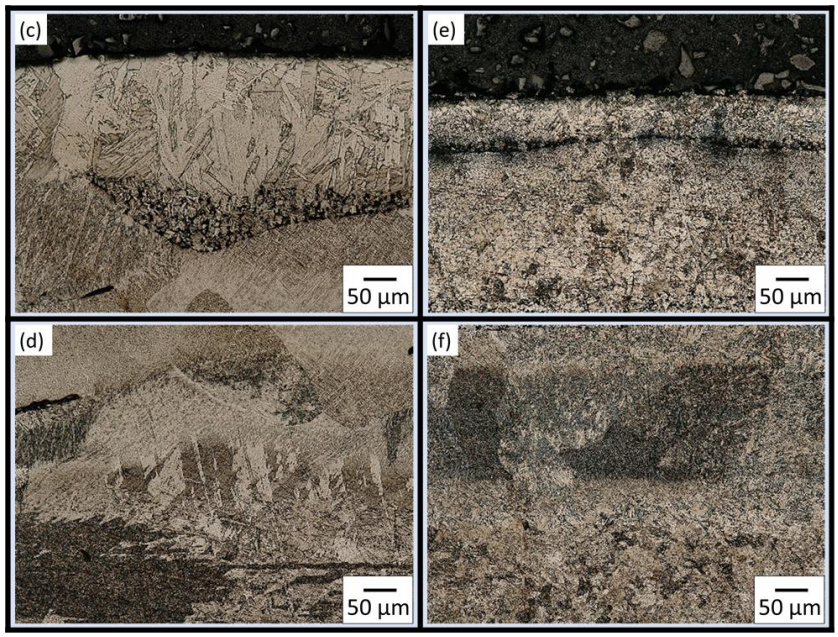

Fig. 11. Higher magnification image of the marked area in (a) and (b) of Fig. 10

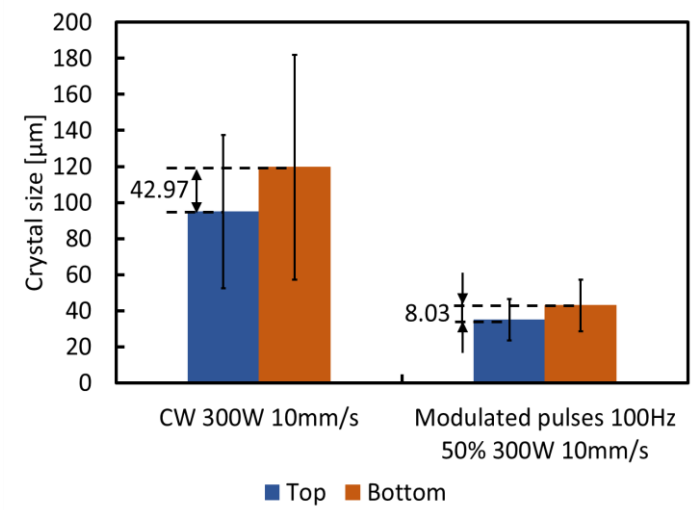

Fig. 12. Grain size near the surface and near the baseplate of fabricated object with CW laser and modulated pulsed laser

4. Discussions

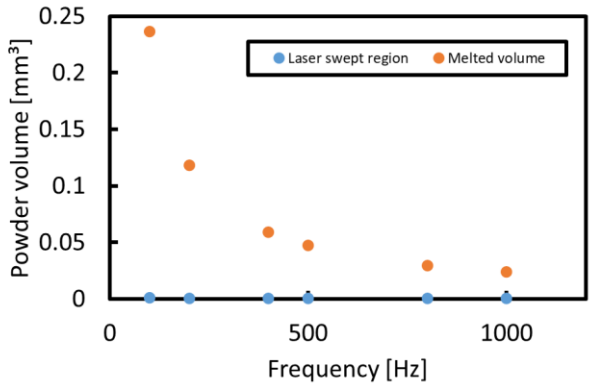

Fig. 13. Amount of powder that can be melted at each frequency and amount of powder at the irradiation point

It was found that as the frequency increased, the surface roughness increased, and the grain size decreased. The laser swept region and melted volume for each frequency were calculated. Figure 13 shows correlation between the laser swept region and the melted volume at each frequency. At the frequency of 100 Hz, the melted volume is 0.24 mm³, and the swept region is 8.93×10^{-4} mm³. Both of these values decrease as the frequency increases, and at a frequency of 1000 Hz, the laser swept region and the melted volume are 2.36×10^{-2} mm³ and 4.43×10^{-4} mm³, respectively. From the above, it can be seen that the change in the melted volume is very large compared to the laser swept region. It was suggested that the increase in the surface roughness is due to the increase in the ratio of the swept region to the melted volume. Similarly, the change in grain size may be due to the change in pulse energy. During the laser irradiation, the heat input to the molten powder is continuous, and the grains grow larger, but as the pulse energy decreases with increasing frequency, the grain size becomes smaller due to the quenching effect.

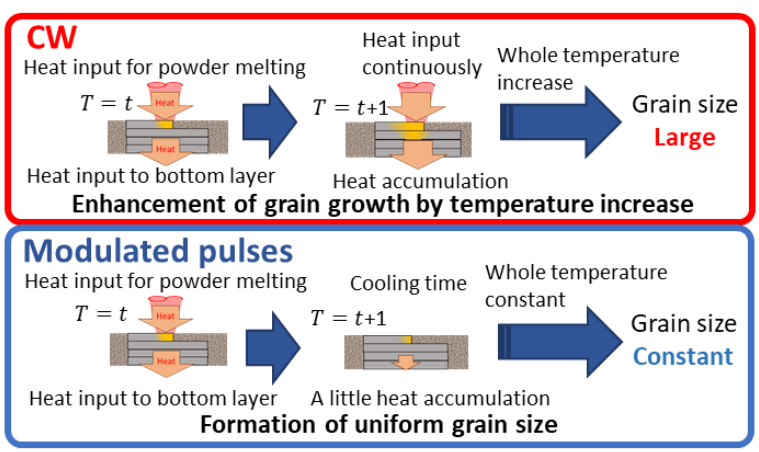

Fig. 14. Schematic diagram of heat input and difference of grain growth with CW laser and modulated pulsed laser

From the 10-layer fabrication experiments, it was clarified that the formed objects using the modulated pulse laser have finer crystal grains inside than those formed by the CW laser, and the difference in the average

grain size between near the surface and near the substrate is smaller. When a CW laser is used, the laser is irradiated continuously. Since the heat input by the laser is constantly occurring, heat accumulation in the bottom. The increase in temperature of the entire fabricated object causes the crystal grains to grow larger. In the case of using a modulated pulse laser, there is a time when the laser is not irradiated and heat input is not performed. Cooling avoids the accumulation of heat at the bottom and suppresses the temperature increasing of the entire object, resulting in a uniform grain size. These results suggest that uniformity of the formed grain size is possible by precisely controlling the heat input of the laser using a modulated pulse laser.

5. Summary

The effect on the grain size of the Ti64 object was studied by controlling the heat input of the laser by using modulated pulses. It was found that small crystal grains were formed as the pulse energy decreased. The results of the reduction of the variation of grain size in the fabricated object using the modulated pulsed laser suggest that the uniformity of grain size can be achieved by controlling the heat input using the modulated pulses.

Acknowledgements

This work was partly supported by JSPS Grants-in-Aid for Scientific Research JP19K05079.

References

Chunlei, Q., Nicholas, J.E. A., Moatas, M. A., 2013. Microstructure and tensile properties of selectively laser-melted and of HIPed laser-melted Ti–6Al–4V, Materials Science and Engineering: A 578, p.230

Gieseke, M., Noelke, C., Kaierle, S., Wesling, V., Haferkamp H, 2013. Selective Laser Melting of Magnesium and Magnesium Alloys, Magnesium technology 2013, p.65

Gu, D., Shen, Y., Lu, Z., 2009. Preparation of TiN-Ti5Si3 in situ composites by selective laser melting, Material Letters 63, p.1577

Gu, D., Shen, Y., Meng, G., 2009. Growth morphologies and mechanisms of TiC grains during Selective Laser Melting of Ti–Al–C composite powder, Material Letters 63, p.2536

Mizuguchi, Y., Sato, Y., Yoshida, N., Tsukamoto, M., 2020. Effect of input energy on hardness and surface quarity in Ti64 by spatter-less SLM with modulated pulse, Journal of Laser Applications 33, 012031

Santos, E., C., Shiomi, M., Osakada, K., Laoui, T., 2006. Rapid manufacturing of metal components by laser forming, International Journal of Mashine Tools and Manufacture 46, p. 1459

Sato, Y., Tsukamoto, M., Masuno, S., Yamashita, Y., Tanigawa, D., Abe, N., 2016. Investigation of the microstructure and surface morphology of a Ti6Al4V plate fabricatied by vacuum selective laser melting, Applied Physics A 122, p.439

Sun, J., Yang, Y., Wang, D., 2013. Mechanical properties of a Ti6Al4V porous structure produced by selective laser melting, Materials & Design 49, p.545

Wang, Y. M., Voisin, T., McKeown, J. T., Ye, J., Calta, N. P., Li, Z., Zeng, Z., Zhang, Y., Chen, W., Roehling, T. T., Ott, R. T., Santala, M. K., Depond, P. J., Matthews, M. J., Hamza, A. V., Zhu, T., 2017. Additively manufactured hierarchical stainless steels with high strength and ductility, Nature Materials 17, p.63

Wang, Z., Guan, K., Gao, M., Li, X., Chen, X., Zeng, X., 2012. The microstructure and mechanical properties of deposited-IN718 by selective laser melting, Journal of Alloy and Compounds 513, p.518

Zhang, B., Eddine, N., Han Lin Liao, F., Coddet, C., 2013. Microstructure and magnetic properties of Fe-Ni alloy fabricated by selective laser melting Fe/Ni miced powders, Journal of Material Science & Technology 29, p.757

Zhang, B., Liao, H., Coddet, C., 2013. Selective laser melting commercially pure Ti under vacuum, Vacuum 95, p.25

Zhang, H., Zhu, H., Qi, T., Hu, Z., Zeng, X., 2016. Selective laser melting of high strength Al–Cu–Mg alloys: Processing, microstructure and mechanical properties, Materials Science and Engineering: A 656, p.47